

Effect of film structure on $\text{CH}_3\text{NH}_3\text{PbI}_3$ perovskite thin films' degradation

Cite as: AIP Advances **11**, 025226 (2021); <https://doi.org/10.1063/5.0030610>

Submitted: 27 September 2020 . Accepted: 19 January 2021 . Published Online: 11 February 2021

F. Khelifaoui, I. Belaidi, N. Attaf, and  M. S. Aida



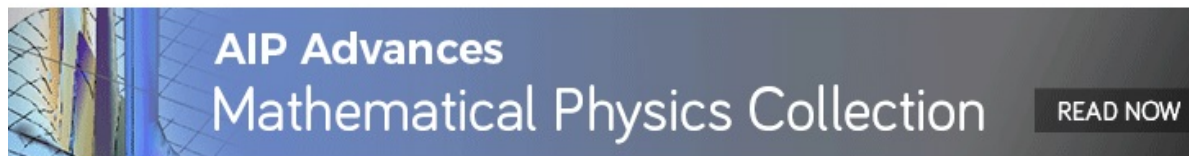
View Online



Export Citation



CrossMark



Effect of film structure on $\text{CH}_3\text{NH}_3\text{PbI}_3$ perovskite thin films' degradation

Cite as: AIP Advances 11, 025226 (2021); doi: 10.1063/5.0030610

Submitted: 27 September 2020 • Accepted: 19 January 2021 •

Published Online: 11 February 2021



View Online



Export Citation



CrossMark

F. Khelifaoui,^{1,2} I. Belaidi,¹ N. Attaf,¹ and M. S. Aida^{3,4,a)} 

AFFILIATIONS

¹Equipe Couche Minces et Environnement, Faculté de Science, Université Frères Mentouri, Constantine 25000, Algeria

²Département de Génie Industriel, Faculté Sciences et Technologie, Université Abbes Laghrour, Khenchela 40000, Algeria

³Department of Physics, Faculty of Science, King Abdulaziz University, Djeddah 21589, Saudi Arabia

⁴Center of Nanotechnology, King Abdulaziz University, Djeddah 21589, Saudi Arabia

^{a)} Author to whom correspondence should be addressed: aida_salah2@yahoo.fr

ABSTRACT

The instability of $\text{CH}_3\text{NH}_3\text{PbI}_3$ perovskite hybrid organic–inorganic films is a serious problem, which might be a drawback for their use in solar energy conversion. In this work, we have evaluated the degradation of the perovskite films and studied the influence of film morphology on their degradation. $\text{CH}_3\text{NH}_3\text{PbI}_3$ perovskite thin films were deposited on glass substrates by a spin coating technique at different centrifugation speeds using different solvents. This study aims to determine the films' properties that may control the degradation process. This study was based on the comparison between the characteristics determined from XRD analysis and optical transmittance of freshly deposited films and those aged 1 year in ambient air at room temperature and dark conditions. The degradation was manifested by the partial decomposition of the perovskite to PbI_2 , I_2 , and metallic lead. The degradation evaluation was achieved by the determination of the variation of the most intense XRD diffraction peak in the freshly prepared film and after aging. The results indicated that the degradation is very sensitive to the films' porosity and thickness. Reducing the thickness of the film or increasing the porosity enhances the degradation process.

© 2021 Author(s). All article content, except where otherwise noted, is licensed under a Creative Commons Attribution (CC BY) license (<http://creativecommons.org/licenses/by/4.0/>). <https://doi.org/10.1063/5.0030610>

INTRODUCTION

During the last decade, the scientific community has paid great attention to organic–inorganic hybrid perovskite materials, which appear as an alternative in photovoltaic applications due to their excellent properties. Among a large variety of perovskite semiconductors, methylammonium lead halide perovskites, $\text{CH}_3\text{NH}_3\text{PbX}$ ($X = \text{Cl}, \text{Br}, \text{and I}$), have emerged as a promising absorbing layer. This material has a tunable direct bandgap in the order of 1.55 eV, an absorption coefficient of 10^5 cm^{-1} in the visible range superior to that of c-Si, and charge carriers' diffusion lengths of 129 nm for electrons and 105 nm for holes, which are ten times larger than those of conventional semiconductors that can reach 1000 nm by introducing chlorine.^{1–4} Earlier, perovskite was used in solar cells based on dye technology.⁵ The low conversion efficiency of 2.19%, achieved with dye perovskite solar cell films, motivated the deposition of perovskite films on mesoporous TiO_2 film, leading to a conversion

efficiency up to 3.81%.⁶ The resolution of perovskite solubility problem in an electrolyte by using hole transporter semiconductor spiro-OMeTAD enables the perovskite solar cells to attain a conversion efficiency of up to 9.7%.⁷

The direction of the planar architecture of perovskite solar cells has been encouraged by the relatively high electron and holes' mobility measured in the planar structure by Stranks *et al.*⁸ Thereafter, intensive research was done to perovskite thin film deposition,^{8–11} yielding a rapid increase in the conversion efficiency that approaches 25%,¹² which becomes comparable to silicon-based solar cells efficiency.

However, this amazing rapid increase in the solar energy conversion obtained by a lead halide perovskite-based solar cell is distressed by the film degradation with aging time.¹³ Indeed, the organic–inorganic hybrid perovskite films also suffer from instability in ambient air, which have repercussions on the performance of solar cells, and this might be a serious drawback for the development

of perovskite-based solar cells. Consequently, this problem has been a relevant stimulus to the perovskite degradation study.^{14,15} However, it is still an open problem since the degradation mechanism has not yet been well understood and resolved.

Nevertheless, two approaches have been suggested to explain the perovskite degradation. Frost *et al.*¹⁶ suggested perovskite decomposition due to the moisture contact, for example, the methylammonium lead triiodide decomposition in HI, PbI₂, and CH₃NH₂. Several authors' investigations have comforted this model.^{15,17,18} More recently, Schoonman¹⁹ suggested the radiation effect as the cause of degradation. In their model, they claimed that the photo-generated holes' migration to the surface is at the origin of reaction with neutral iodine, leading to the degradation of the perovskite. Similar ionization stimulated degradation model has been proposed by Oksengendler *et al.*²⁰

The whole degradation studies were carried out on the effect of environmental conditions on the perovskite degradation such as heat, UV radiation, and moisture.^{21–23} In general, the degradation studies are focused only on moisture, oxygen, and light. Abdelmageed *et al.*²⁴ investigated the perovskite degradation with light in an inert atmosphere. Regarding the proposed degradation models, the surface of the film plays a key role in degradation, since the degradation reactions and decomposition occur in this region, i.e., the film's open surface. Consequently, the film morphology and porosity may influence the degradation kinetics. To the best of our knowledge, there is no report on the effect of film structure and morphology on the degradation process.

Several perovskite thin film deposition techniques have been used, such as spin-coating process,^{25,26} doctor blade,²⁷ vapor-assisted solution process,^{28,29} and ultrasonic spray deposition.^{30,31} The synthesis procedure of CH₃NH₃PbI₃ perovskite using spin coating can be achieved through two methods: one-step through spin-coating of CH₃NH₃I and PbI₂ solution mixture followed by film annealing or two-step processes based on spin-coating of a PbI₂ film followed by the film dipping into a CH₃NH₃I solution.^{32,33}

Perovskite thin films, prepared on a flat substrate by spin coating technique, are characterized by a highly rough and porous surface.³⁴

In this work, we studied the degradation of spin-coated CH₃NH₃PbI₃ perovskite films and investigated the effect of deposition parameters, such as centrifugation speed and solvent nature, on the film degradation. The films were characterized once freshly prepared and after 1 year of aging in the dark at room temperature.

EXPERIMENTAL DETAILS

Methylammonium lead iodine perovskite thin films were deposited on glass substrates in ambient air at room temperature by a spin coating method. The starting solution is a mixture of an equimolar solution of PbI₂ and CH₃NH₃I. In this study, we used two kinds of solvents: DMF (*N,N*-dimethylformamide) and a mixture of DMF and DMSO (dimethyl sulfoxide). The obtained solution was stirred at 60 °C and immediately kept in dark at room temperature for 24 h. During film formation, various centrifugation speeds (750 rpm–2000 rpm) were used. Subsequently, the freshly deposited films were annealed at a low temperature of 70 °C for 30 min, and the low annealing temperature is used to avoid

CH₃NH₃I exodiffusion.³⁵ More experimental details are mentioned in our previous work.³⁴

The surface morphology of the films was examined using a Horiba Scientific JSM-7100 scanning electron microscope. The structural properties of the films were analyzed using XRD using Philips X'Pert System with CuK α radiation ($\lambda = 1.5418 \text{ \AA}$). The optical properties were investigated using a double-beam spectrophotometer (Shimadzu 3100S).

The films were characterized after deposition and after 1-year storage in dark at ambient temperature and humidity in order to study the film degradation.

RESULTS AND DISCUSSION

Figure 1 represents the micrographs of the freshly deposited film [Fig. 1(a)] and after 1-year aging [Fig. 2(b)]. The film color varies from dark as deposited to yellowish after aging. This is clear evidence of the perovskite film degradation with time and a primary evaluation of this phenomenon. The humid atmosphere accelerates film degradation. Al Mamun *et al.*²¹ observed the film color variation from black to yellow and no perovskite phase after exposure to air for more than 66 h at 40% humidity. Ouafi *et al.*³⁶ noticed that CH₃NH₃PbI₃ perovskite films start degradation after 3 h of UV light exposure to reach a complete degradation after 12 h. Li *et al.*³⁷ reported the CH₃NH₃PbI₃ perovskite degradation under intense UV and vacuum. To exclude the effect of air and humidity, recently, Abdelmageed *et al.*²⁴ aged CH₃NH₃PbI₃ perovskite under intense solar radiation and elevated temperature, and they noticed that the film starts to degrade above 75 °C and at 95 °C in dark. According to this, three factors may control the CH₃NH₃PbI₃ perovskite degradation: the humidity, the light exposure, and the air contact and their combination. The light exposure and humidity accelerate the CH₃NH₃PbI₃ perovskite degradation.

Figures 2(a) and 2(b) show the UV visible transmissions of perovskite films, prepared with two different solvents, freshly deposited and after 1-year aging. As can be seen, after aging, the films have larger transparency in the whole visible range when compared to their initial transmission. The transmittance increases from 10% to 20% after aging, which is consistent with the films' micrograph (Fig. 1).

For more insight on the films' degradation, we have analyzed the film composition variation by recording the XRD pattern of CH₃NH₃PbI₃ perovskite films, freshly prepared films with different solvent and spinning speed conditions, and after aging (Figs. 3 and 4). All films are polycrystalline, and the XRD patterns of fresh samples are composed of different diffraction peaks assigned to the planes (110), (200), (202) (220), (320), (312), (224), (330), and (404)

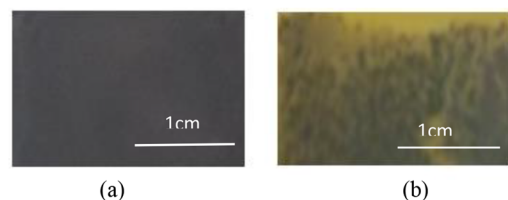
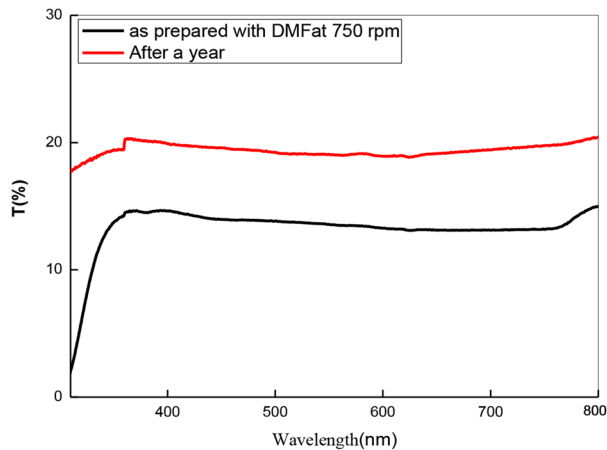
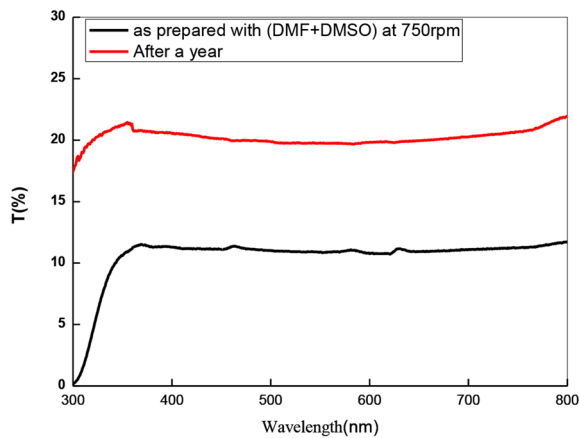


FIG. 1. Photographic image of (a) freshly prepared perovskite film and (b) after aging.



(a)



(b)

FIG. 2. Optical transmission in the visible range of freshly prepared perovskite film after aging measured in films prepared using (a) DMF solvent and (b) DMF + DMSO mixture solvent.

of the tetragonal structure of $\text{CH}_3\text{NH}_3\text{PbI}_3$ perovskite. There is no noticeable difference between the patterns of films prepared with the different solvents except that the diffraction peaks of the mixed solution are more intense, which is probably due to the increase in the films' thickness. In addition, a slight reduction in the peaks' intensities with the increase in the spinning velocity is observed also due to the reduction in films' thickness. The DRX pattern of the film after 1-year of aging revealed the decrease in perovskite phase peaks and the emergence of new peaks assigned to the hexagonal PbI_2 phase, lead metallic phase, and I_2 phase, as shown in Figs. 3 and 4. Several authors have mentioned that the perovskite degradation is characterized by the reduction in the perovskite peaks intensity to total

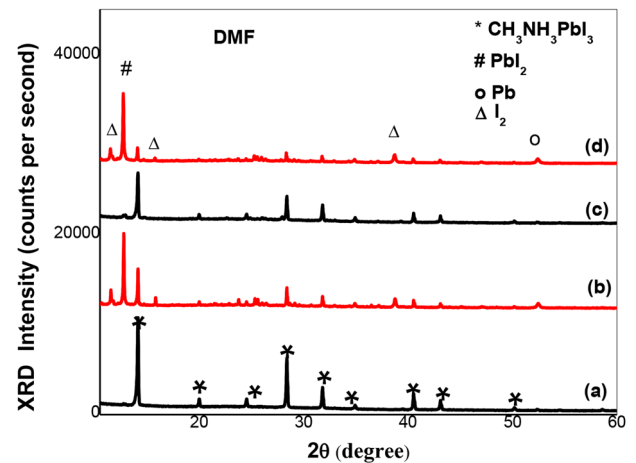


FIG. 3. XRD diffraction patterns of freshly prepared perovskite film after aging measured in films prepared using DMF as solvent with different spinning speeds—750 rpm: (a) as prepared and (b) after aging and 1000 rpm; (c) as grown and (d) after aging.

disappearance and the emergence of peaks related to PbI_2 , metallic lead,²⁴ and iodine phases.^{21,38} In our case, the perovskite was partially converted to PbI_2 confirmed by the peaks located at the angles— 12.6° and 38.6° , to metallic Pb characterized by the peak located at 52.3° , and to a noticeable orthorhombic I_2 phase characterized by the peaks located at 11.56° and 38.7° . An interesting feature is that the films are not totally degraded, since the films were stored in dark. This may suggest that the effect of light exposure is more crucial for perovskite degradation than the air. Li *et al.*³⁷ have investigated the $\text{CH}_3\text{CH}_3\text{PbI}_3$ perovskite degradation under blue light, and they concluded that the perovskite degradation is more sensitive to the laser radiation rather than to the heating effect of laser.

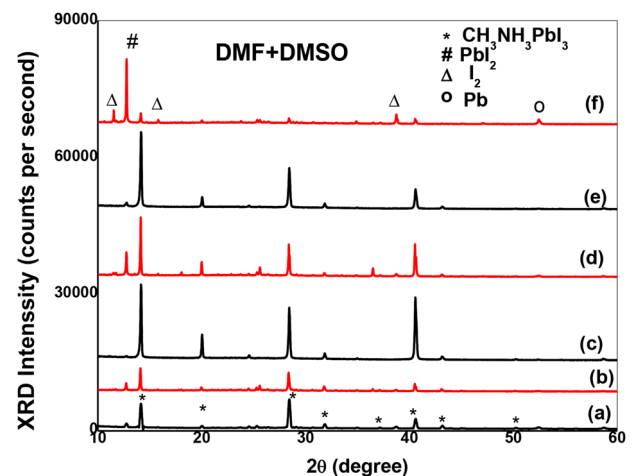


FIG. 4. XRD diffraction patterns of freshly prepared perovskite film after aging measured in films prepared using DMF + DMSO mixture as solvent with different spinning speeds—750 rpm: (a) as prepared and (b) after aging; 1000 rpm: (c) as grown and (d) after aging; and 2000 rpm: (e) as grown and (f) after aging.

TABLE I. Deposition conditions, thickness, and porosity of different perovskite properties of $\text{CH}_3\text{NH}_3\text{PbI}_3$ perovskite thin films.

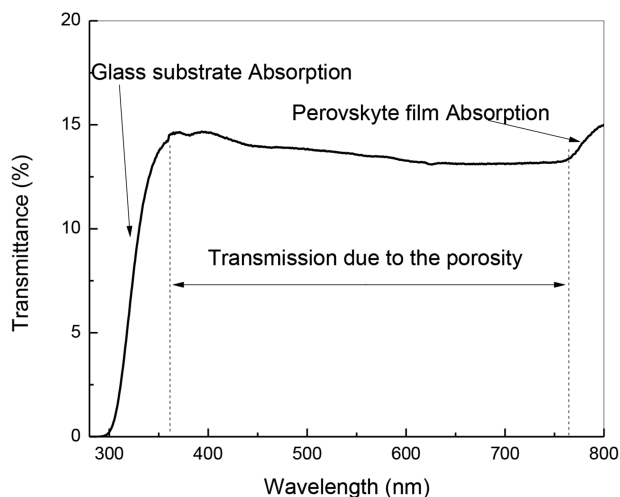
	Spinning speed (rpm)	Thickness (nm)	Porosity (%)
DMF solvent	750	1070.33	13.20
	1000	858.00	24.80
DMF + DMSO mixture solvent	750	2591.33	11.25
	1000	1576.33	25.70
	2000	703	24.80

The degradation mechanism of perovskite is still an open problem and is currently under continuous debate.³⁹ The general agreement is that the perovskite degradation mechanism is based on the material decomposition in different phases: HI, PbI_2 , Pb, I_2 , and volatile organic compound CH_3NH_2 . The degradation is activated by agents such as water, oxygen,⁴⁰ and ultraviolet light.⁴¹

In the photonic model, the photogenerated holes' migration to the surface is at the origin of reaction with neutral iodine, leading to the degradation of the perovskite.²⁰

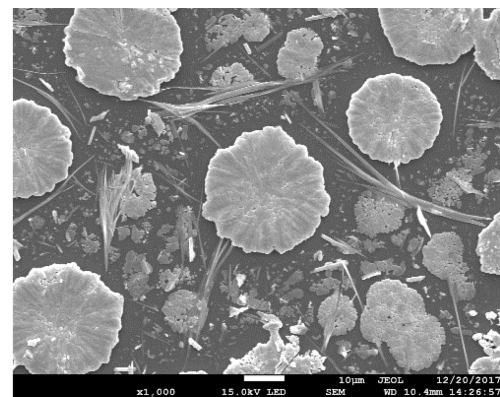
For the degradation in a humid atmosphere, several authors³⁸ suggested H_2O as a catalyzer. H_2O reacts with perovskite in darkness, forming a hydrate product as the first step of the degradation process. It is well argued that O_2 plays a crucial role in the degradation of perovskite, where free radicals, such as superoxides, are generated and subsequently interact with the organic cation of the perovskite molecule, which leads to the degradation to PbI_2 .^{40,42,43}

In general, regardless of the degradation agent, the decomposition occurs on the film's surface. Consequently, the larger the free surface (i.e., larger surface contact with water, air, and light), the important the degradation. Thereafter, the film morphology and porosity may play an important role in the perovskite films' degradation. In Table I, the films' characteristics, such as thickness,

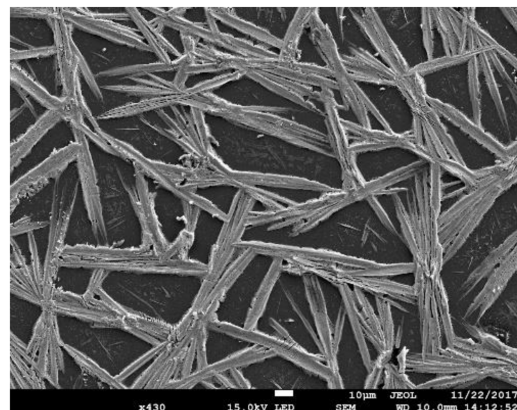
**FIG. 5.** Typical transmission spectrum of perovskite film in the UV-visible range showing the porosity contribution used for films' porosity estimation.

porosity, and bandgap values, measured in films prepared with different conditions are summarized. The porosity was estimated from UV-visible transmittance spectra of the films. More details are reported in a previous paper,³⁴ where the films' porosity was estimated from the film transmittance plateau value. Indeed, perovskite thin film deposited on glass exhibits two absorption edges: (i) at the low photon energy corresponding to the perovskite gap and (ii) at the higher photon energy corresponding to the glass substrate absorption edge. The transmittance plateau between these two edges is due to the porosity in the film, as depicted in Fig. 5.

As reported in Table I, the films are characterized by a large porosity up to 25%, and the deposition parameters, such as solvent nature and spinning speed, control the films' porosity, as can be concluded from Table I. The SEM images [Figs. 6(a) and 6(b)] reveal the large porosity of the prepared films. The prepared films are not continuous and they exhibit various morphologies, as shown in Figs. 6(a) and 6(b). The film prepared with DMF solvent is composed of a "flower like" structure, randomly dispersed with a variable size, while the film prepared with the solvent mixture DMF and DMSO exhibits a structure composed of elongated fibers or wires.



(a)



(b)

FIG. 6. SEM images of perovskite $\text{CH}_3\text{NH}_3\text{PbI}_3$ films deposited at 1000 rpm spinning speed using (a) DMF solvent and (b) mixture solvent.

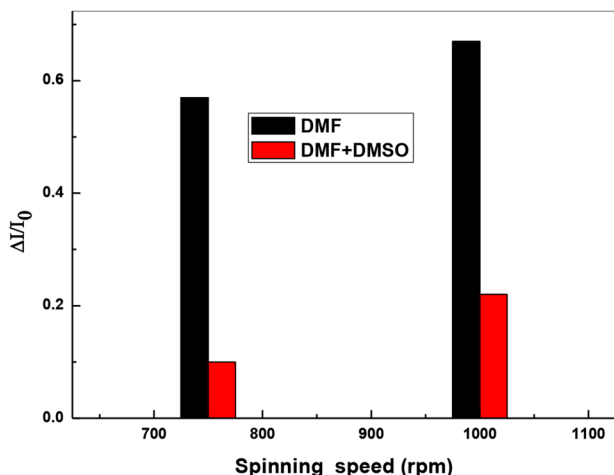


FIG. 7. Histogram showing the degradation ratio measured in film prepared with two different solvents and spinning speeds.

To evaluate the films' degradation rate, we have calculated the relative difference in the intensity of the most intense peak characterizing perovskite located at the angle 14.04° assigned to the (110) diffraction plane of the tetragonal $\text{CH}_3\text{NH}_3\text{PbI}_3$ phase,

$$\Delta I/I_0 = (I_0 - I)/I_0,$$

where I_0 and I are the peak intensities measured in freshly deposited film and after 1-year aging, respectively.

As discussed earlier, the presence of surface porosity offers more available surface reaction; moreover, the thinner film allows

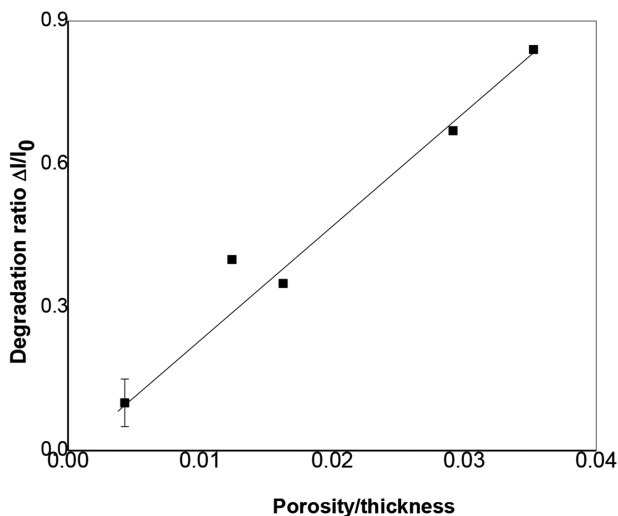


FIG. 8. Variation of the degradation ($\Delta I/I_0$) as a function of the (P/d) quantity, where P is the film porosity and d is the film thickness.

the light, oxygen, and humidity diffusion in the film network. Consequently, increasing the surface porosity and reducing the film thickness may enhance the degradation process. In Fig. 7, we have plotted a histogram showing the values of the degradation ratio of films prepared by solvent DMF and a mixture of DMF and DMSO with two different spinning speeds. The film prepared with DMF and a high spinning speed of 1000 rpm exhibits the highest degradation ratio; this is due to the combination of its low thickness and relatively high porosity, whereas the film prepared with DMF and DMSO solvent mixture and a low spinning speed of 750 rpm is more stable due to its large thickness and low porosity (Table I).

The degradation ratio is then proportional to the porosity and inversely proportional to the thickness. Therefore, we have plotted (Fig. 8) the degradation ratio variation as a function of the ratio porosity/thickness. As can be seen, the perovskite degradation ratio varies linearly with porosity/thickness quantity. This indicates that besides the external environmental conditions (air, light, and humidity), the internal structural properties of the film, including thickness and porosity, play an important role in perovskite degradation.

CONCLUSION

In this work, we have investigated the impact of deposition parameters and properties on perovskite films' stability. The films were prepared using different solvents and deposited at different speed rotations by the spin coating technique. The perovskite degradation was evaluated by the comparison between the structural and optical properties of freshly prepared film and after aging. The perovskite $\text{CH}_3\text{NH}_3\text{PbI}_3$ film degradation is characterized by the change of film color from black to yellow and by the increase in optical transmittance after aging. The XRD analysis reveals the partial decomposition of the perovskite to different phases such as PbI_2 , I_2 , and Pb . The degradation of the films was evaluated by the relative ratio of the difference between the most peak of perovskite intensities in both freshly prepared film and after aging. We concluded that the film porosity and thickness play a key role in the degradation ratio. Thinner and highly porous films undergo larger degradation.

ACKNOWLEDGMENTS

The authors declare that they have no conflict of interest.

DATA AVAILABILITY

The data that support the findings of this study are available from the corresponding author upon reasonable request.

REFERENCES

- C. C. Stoumpos, C. D. Malliakas, and M. G. Kanatzidis, "Semiconducting tin and lead iodide perovskites with organic cations: Phase transitions, high mobilities, and near-infrared photoluminescent properties," *Inorg. Chem.* **52**, 9019 (2013).
- G. Xing, N. Mathews, S. Sun, S. S. Lim, Y. M. Lam, M. Gratzel, S. Sun, and T. C. Mhaisalkar, "Long-range balanced electron- and hole-transport lengths in organic-inorganic $\text{CH}_3\text{NH}_3\text{PbI}_3$," *Science* **342**, 344 (2013).

- ³S. D. Stranks, G. E. Eperon, G. Grancini, C. Menelaou, M. J. P. Alcocer, T. Leijtens, L. M. Herz, A. Petrozza, and H. J. Snaith, "Electron-hole diffusion lengths exceeding 1 micrometer in an organometal trihalide perovskite absorber," *Science* **342**, 341 (2013).
- ⁴Y. Zhao, A. M. Nardes, and K. Zhu, "Solid-state mesostructured perovskite $\text{CH}_3\text{NH}_3\text{PbI}_3$ solar cells: Charge transport, recombination, and diffusion length," *J. Phys. Chem. Lett.* **5**, 490 (2014).
- ⁵A. Kojima, K. Teshima, T. Miyasaka, and Y. Shirai, "Novel photoelectrochemical cell with mesoscopic electrodes sensitized by lead-halide compounds," in 2nd Proceedings of the 10th ECS, 2006.
- ⁶A. Kojima, K. Teshima, Y. Shirai, and T. Miyasaka, "Organometal halide perovskites as visible-light sensitizers for photovoltaic cells," *J. Am. Chem. Soc.* **131**, 6050 (2009).
- ⁷H. S. Kim, C. R. Lee, J. H. Yum, J. E. Moser, M. Grätzel, and N. G. Park, "Lead iodide perovskite sensitized all-solid-state submicron thin film mesoscopic solar cell with efficiency exceeding 9%," *Sci. Rep.* **2**, 591 (2012).
- ⁸J. Burschka, N. Pellet, S.-J. Moon, K. H. Baker, P. Gao, M. K. Nazeeruddin, and M. Grätzel, "Sequential deposition as a route to high-performance perovskite-sensitized solar cells," *Nature* **499**, 316 (2013).
- ⁹M. Liu, M. B. Johnston, and H. J. Snaith, "Efficient planar heterojunction perovskite solar cells by vapour deposition," *Nature* **501**, 395 (2013).
- ¹⁰Q. Chen, H. Zhou, Z. Hong, S. LuO, H.-S. Duan, H.-H. Wang, Y. Liu, G. Li, and Y. Yang, "Planar heterojunction perovskite solar cells via vapor-assisted solution process," *J. Am. Chem. Soc.* **136**(2), 622 (2014).
- ¹¹Y. Zhao and K. Zhu, "Three-step sequential solution deposition of PbI_2 -free $\text{CH}_3\text{NH}_3\text{PbI}_3$ perovskite," *J. Mater. Chem. A* **3**, 9086 (2015).
- ¹²H. J. Snaith, "Perovskites: The emergence of a new era for low-cost, high-efficiency solar cells," *J. Phys. Chem. Lett.* **4**, 3623 (2013).
- ¹³T. Leijtens, G. E. Eperon, S. Pathak, A. Abate, M. M. Lee, and H. J. Snaith, "Overcoming ultraviolet light instability of sensitized TiO_2 with meso-structured organometal tri-halide perovskite solar cells," *Nat. Commun.* **4**, 2885 (2013).
- ¹⁴N. Ashurov, B. L. Oksengendler, S. Maksimov, S. Rashidova, A. R. Ishteev, D. S. Saranin, I. N. Burmistrov, D. V. Kuznetsov, and A. A. Zakhisov, "Current state and perspectives for organo-halide perovskite solar cells. Part 1. Crystal structures and thin film formation, morphology, processing, degradation, stability improvement by carbon nanotubes. A review," *Mod. Electron. Mater.* **3**, 1 (2017).
- ¹⁵C. Wang, Y. Li, X. Xu, C. Wang, F. Xie, and Y. Gao, "Chemical interaction dictated energy level alignment at the $\text{N,N}'$ -dipentyl-3,4,9,10-perylene-dicarboximide/ $\text{CH}_3\text{NH}_3\text{PbI}_3$ interface," *Chem. Phys. Lett.* **649**, 151 (2016).
- ¹⁶J. M. Frost, K. T. Butler, F. Brivio, C. H. Hendon, M. van Schilfhaarde, and A. Walsh, "Atomistic origins of high-performance in hybrid halide perovskite solar cells," *Nano Lett.* **14**, 2584 (2014).
- ¹⁷J. A. Christians, P. A. M. Herrera, and P. V. Kamat, "Transformation of the excited state and photovoltaic efficiency of $\text{CH}_3\text{NH}_3\text{PbI}_3$ perovskite upon controlled exposure to humidified air," *J. Am. Chem. Soc.* **137**, 1530 (2015).
- ¹⁸J. Yang, B. D. Siempelkamp, D. Liu, and T. L. Kelly, "Investigation of $\text{CH}_3\text{NH}_3\text{PbI}_3$ degradation rates and mechanisms in controlled humidity environments using in situ techniques," *ACS Nano* **9**, 1955 (2015).
- ¹⁹J. Schoonman, "Organic-inorganic lead halide perovskite solar cell materials: A possible stability problem," *Chem. Phys. Lett.* **619**, 193 (2015).
- ²⁰B. L. Oksengendler, O. B. Ismailova, M. B. Marasulov, and I. Z. Urolov, "On the degradation mechanism of functioning solar cells based on organic-inorganic perovskites," *Appl. Sol. Energy* **50**, 255 (2014).
- ²¹A. Al Mamun, Y. Mohammed, T. T. Ava, G. Namkoong, and A. A. Elmustafa, "Influence of air degradation on morphology, crystal size and mechanical hardness of perovskite film," *Mater. Lett.* **229**, 167 (2018).
- ²²H. Oga, A. Saeki, Y. Ogomi, S. Hayase, and S. Seki, "Improved understanding of the electronic and energetic landscapes of perovskite solar cells: High local charge carrier mobility, reduced recombination, and extremely shallow traps," *J. Am. Chem. Soc.* **136**, 13818 (2014).
- ²³F.-S. Zu, P. Amsalem, I. Salzmann, R.-B. Wang, M. Ralairisova, S. Kowarik, S. Duhm, and N. Koch, "Impact of white light illumination on the electronic and chemical structures of mixed halide and single crystal perovskites," *Adv. Opt. Mater.* **5**, 1700139 (2017).
- ²⁴G. Abdelmageed, C. Mackeen, K. Hellier, L. Jewell, L. Seymour, M. Tingwald, F. Bridges, J. Z. Zhang, and S. Carter, "Effect of temperature on light induced degradation in methylammonium lead iodide perovskite thin films and solar cells," *Sol. Energy Mater. Sol. Cells* **174**, 566 (2018).
- ²⁵M. M. Tavakoli, L. Gu, Y. Gao, C. Reckmeier, J. He, A. L. Rogach, Y. Yao, and Z. Fan, "Fabrication of efficient planar perovskite solar cells using a one-step chemical vapor deposition method," *Sci. Rep.* **5**, 14083 (2015).
- ²⁶F. Wang, D. Meng, X. Li, Z. Zhu, Z. Fu, and Y. Lu, "Influence of annealing temperature on the crystallization and ferroelectricity of perovskite $\text{CH}_3\text{NH}_3\text{PbI}_3$ film," *Appl. Surf. Sci.* **357**, 391 (2015).
- ²⁷Y. Deng, E. Peng, Y. Shao, Z. Xiao, Q. Dong, and J. Huang, "High efficiency flexible perovskite solar cells using superior low temperature TiO_2 ," *Energy Environ. Sci.* **8**, 1544 (2015).
- ²⁸L. K. Ono, M. R. Leyden, S. Wang, and Y. Qi, "Organometal halide perovskite thin films and solar cells by vapor deposition," *J. Mater. Chem. A* **4**, 6693 (2016).
- ²⁹X. Ren, Z. Yang, D. Yang, X. Zhang, D. Cui, Y. Liu, Q. Wei, H. Fan, and S. F. Liu, "Modulating crystal grain size and optoelectronic properties of perovskite films for solar cells by reaction temperature," *Nanoscale* **8**, 3816 (2016).
- ³⁰J. G. Tait, S. Manghooli, W. Qiu, L. Rakocevic, L. Kootstra, M. Jaysankar, C. A. Masse de la Huerta, U. W. Paetzold, R. Gehlhaar, D. Cheyens, P. Heremans, and J. Poortmans, "Rapid composition screening for perovskite photovoltaics via concurrently pumped ultrasonic spray coating," *J. Mater. Chem. A* **4**, 3792 (2016).
- ³¹H. Huang, J. Shi, L. Zhu, D. Li, Y. Luo, and Q. Meng, "Two-steps ultrasonic spray deposition of $\text{CH}_3\text{NH}_3\text{PbI}_3$ for efficient and large area perovskite solar cell," *Nano Energy* **27**, 352 (2016).
- ³²J.-H. Im, I.-H. Jang, N. Pellet, M. Grätzel, and N.-G. Park, "Growth of $\text{CH}_3\text{NH}_3\text{PbI}_3$ cuboids with controlled size for high-efficiency perovskite solar cells," *Nat. Nanotechnol.* **9**, 927 (2014).
- ³³B.-E. Cohen and L. Etgar, "Parameters that control and influence the organometal halide perovskite crystallization and morphology," *Front. Optoelectron.* **9**, 44 (2016).
- ³⁴I. Belaidi, F. Khelfaoui, N. Attaf, A. Azzizi, and M. S. Aida, "Solvent and spinning speed effects on $\text{CH}_3\text{NH}_3\text{PbI}_3$ films deposited by spin coating," *Phys. Status Solidi A* **216**, 1900340 (2019).
- ³⁵W. Zhang, S. Pathak, N. Sakai, T. Stergiopoulos, P. K. Nayak, K. Nakita, N. K. Noel, A. A. Haghighirad, M. Victor, V. M. Burlakov, D. W. deQuilettes, A. Sadhanala, W. Li, L. Liduo Wang, S. David, D. S. Ginger, R. H. Friend, and H. J. Snaith, "Enhanced optoelectronic quality of perovskite thin films with hypophosphorous acid for planar heterojunction solar cells," *Nat. Commun.* **6**, 10030 (2015).
- ³⁶M. Ouafi, B. Jaber, L. Atourki, R. Bekkari, and L. Laanab, "Improving UV stability of MAPbI_3 perovskite thin films by bromide incorporation," *J. Alloys Compd.* **746**, 391 (2018).
- ³⁷Y. Li, X. Xu, C. Wang, B. Ecker, J. Yang, J. Huang, and Y. Gao, "Light-induced degradation of $\text{CH}_3\text{NH}_3\text{PbI}_3$ hybrid perovskite thin film," *J. Phys. Chem. C* **121**, 3904 (2017).
- ³⁸G. Niu, W. Li, F. Meng, L. Wang, H. Dong, and Y. Qiu, "Study on the stability of $\text{CH}_3\text{NH}_3\text{PbI}_3$ films and the effect of post-modification by aluminum oxide in all-solid-state hybrid solar cells," *J. Mater. Chem.* **2**, 705 (2013).
- ³⁹N. H. Nickel, F. Lang, V. V. Brus, O. Shargaieva, and J. Rappich, "Influence of radiation on the properties and the stability of hybrid perovskites," *Adv. Electron. Mater.* **3**, 1700158 (2017).
- ⁴⁰D. Bryant, N. Aristidou, S. Pont, I. Sanchez-Molina, T. Chotchuangchuchaval, S. Wheeler, J. R. Durranta, and S. A. Haque, "Light and oxygen induced degradation limits the operational stability of methylammonium lead triiodide perovskite solar cells," *Energy Environ. Sci.* **9**, 11850 (2016).
- ⁴¹S. Lee, S. Kim, S. Bae, K. Cho, T. Chung, L. Mundt, S. Lee, S. Park, H. Park, M. C. Schubert, S. W. Glunz, Y. Ko, Y. Jun, Y. Kang, H. S. Lee, and D. Kim, "UV degradation and recovery of perovskite solar cells," *Sci. Rep.* **6**, 38150 (2016).

⁴²G. Abdelmageed, L. Jewell, K. Hellier, L. Seymour, B. Luo, F. Bridges, J. Z. Zhang, and S. Carter, "Mechanisms for light induced degradation in MAPbI₃ perovskite thin films and solar cells," *Appl. Phys. Lett.* **109**, 233905 (2016).

⁴³N. Aristidou, I. Sanchez-Molina, T. Chotchuangchutchaval, M. Brown, L. Martinez, T. Rath, and S. A. Haque, "The role of oxygen in the degradation of methylammonium lead trihalide perovskite photoactive layers," *Angew. Chem., Int. Ed.* **54**, 8208 (2015).